XVII CONGRESO INTERNACIONAL
Expresión Gráfica Aplicada a la Edificación
APEGA CARTAGENA 2025
PENSAMIENTO GRÁFICO
OCTUBRE
02 | 03 | 04

How to cite: Capetillo-Ordaz, N.B.; Bernal López-Sanvicente, A.; Alonso-Tristán, C.; Beckers, B.. BRIDGING REALITY AND SIMULATION: LIDAR VS. PHOTOGRAMMETRY FOR FEM-READY BIM MODELS. Graphic thinking. Proceedings of XVII INTERNATIONAL CONFERENCE ON GRAPHIC EXPRESSION APPLIED TO BUILDING – APEGA CARTAGENA 2025. Cartagena, october 2, 3 and 4, 2025. pp. 548-559.

# BRIDGING REALITY AND SIMULATION: LIDAR VS. PHOTOGRAMMETRY FOR FEM-READY BIM MODELS

Nayely B. Capetillo-Ordaz. SWIFT Research Group, University of Burgos
nbcapetillo@ubu.es
Escuela Politécnica Superior, Río Vena. Avda. Cantabria, s/n, 09006, Burgos, Spain

Amparo Bernal López-Sanvicente. University of Burgos
amberlop@ubu.es
Escuela Politécnica Superior, Milanera. Calle Villadiego, s/n, 09001, Burgos, Spain

Cristina Alonso-Tristán. SWIFT Research Group, University of Burgos
catristan@ubu.es
Escuela Politécnica Superior, Río Vena. Avda. Cantabria, s/n, 09006, Burgos, Spain

Benoit Beckers. Urban Physics Joint Laboratory, Université de Pau et des Pays de l'Adour
benoit.beckers@univ-pau.fr
Allée du Parc Montaury, 64600, Anglet, France

## Abstract

Through a case study of the Higher Polytechnic School at the University of Burgos, this study compares two point cloud acquisition methods: photogrammetry and LiDAR. The objective is to evaluate which technique offers higher geometric fidelity and suitability for downstream thermal simulation workflows.

A dense photogrammetric point cloud was generated using images captured with a Canon EOS R5 mounted on an aerial pole and processed in Agisoft Metashape. In parallel, a terrestrial LiDAR scan was acquired using a Leica BLK360 and processed with Autodesk ReCap Pro. Both datasets were analyzed and compared in CloudCompare, using the LiDAR scan as the geometric reference.

The analysis focused on detail accuracy, noise levels, and occlusions. While photogrammetry delivered strong visual detail, particularly on flat surfaces, the LiDAR scan exhibited superior geometric consistency across the full façade. Based on these findings, a high-level-of-detail BIM model was manually reconstructed and embedded with a conformal mesh suitable for finite element method thermal simulations.

This methodology supports the optimization of reality capture workflows for architectural applications, emphasizing the importance of mesh readiness and graphical fidelity in generating accurate, simulation-ready models for environmental analysis.

**Keywords:** Photogrammetry, Graphic Expression, Finite Element Method, Thermal Simulation.

## 1. Introduction

In the pursuit of sustainable architecture, understanding how buildings interact with their surrounding conditions is essential to optimizing energy performance. Among the various tools available, thermal simulations, particularly those based on the finite element method (FEM), provide detailed insights into heat transfer dynamics across building envelopes (Aguerre et al., 2019). However, the accuracy of these simulations depends heavily on the quality of the input geometric models (Muñumer et al., 2022).

Recent advancements in reality capture technologies, such as photogrammetry and laser scanning, have made it increasingly feasible to generate high-fidelity 3D representations of existing buildings rapidly and cost-effectively (Bouziani et al., 2021). These technologies are progressively being integrated into architectural and engineering workflows, for example, to support building performance evaluations (O'Donnell, et al., 2019; Waqar et al., 2025), digital twin development (Brock et al., 2021; Wibisana et al., 2024), and heritage preservation (Partama et al., 2025; Liu et al., 2024).

Photogrammetry, for instance, is a widely adopted reality capture technique that reconstructs three-dimensional geometry from overlapping two-dimensional images. It is particularly accessible and cost-effective, as it can be implemented using consumer-grade equipment, including DSLR cameras or drone-mounted sensors. The reconstruction process involves detecting and matching key points across multiple images to triangulate depth and spatial relationships, employing computer vision algorithms such as Structure from Motion and Multi-View Stereo (Apollonio et al., 2021).

Similarly, Light Detection and Ranging (LiDAR) is an active sensing technology that calculates the distance to surrounding surfaces by emitting laser pulses and measuring the time it takes for them to return (Guan et al., 2022). This process enables the direct acquisition of precise spatial coordinates, resulting in highly accurate 3D point clouds (Guan et al., 2022). While more expensive and specialized than photogrammetry, LiDAR scanners are particularly effective at capturing detailed, hard-to-reach areas and geometrically complex elements and are notably less sensitive to varying lighting conditions compared to image-based methods (Yucel et al., 2024). Additionally, LiDAR captures surrounding context like terrain, vegetation, and unplanned architectural additions, which are often missing from blueprints.

### 1.1. Structured geometry for thermal modeling

While both photogrammetric and LiDAR data offer high-resolution real-world geometries, the challenge lies in transforming these representations into solid, volumetric, simulation-ready models suitable for the finite element method (FEM). This numerical technique solves partial differential equations over discretized domains, enabling the analysis of physical phenomena such as thermal conduction in buildings (Aguerre et al., 2020; Beckers, 2016). FEM subdivides a domain into discrete, finite elements (e.g., hexahedrons or tetrahedrons) (Wolters et al., 2007), enabling the computation of temperature gradients, heat flow, and thermal resistance across complex geometries and materials.

Unlike simplified models that rely on lumped parameters or linear approximations, FEM captures localized effects such as thermal bridges and corner losses, making it ideal for high-resolution architectural simulations (Aguerre et al., 2019). However, its effectiveness depends heavily on the quality of the geometric model and the mesh used for discretization (Wolters et al., 2007). Reality capture technologies often produce noisy, non-manifold, or unstructured geometries (Shan et al., 2021; Zhang et al., 2024) that provide only surface data, lacking explicit information on the

thicknesses of walls, roofs, or slabs. This absence complicates mesh generation and can compromise simulation results. This gap between raw captured data and simulation-ready geometry poses a persistent challenge in applying FEM to existing buildings.

To address this gap, the present study evaluates the geometric fidelity and modeling suitability of data derived from photogrammetry and LiDAR. The goal is to establish a robust and structured foundation for future FEM-based thermal analysis by embedding simulation-ready geometry within a building information modeling (BIM) environment, through a case study of the University of Burgos in Spain. While thermal simulation is not part of this investigation, the resulting model is specifically optimized for such analyses in future research.

## 2. Methodology

The methodological workflow, illustrated in (Fig. 1), outlines the steps followed to evaluate the geometric fidelity of reality capture techniques and to generate a BIM model embedded with structured meshing. The process begins with data acquisition of the study area using two capture methods: high-resolution photogrammetry, conducted with a Canon EOS R5 camera, and terrestrial laser scanning, performed with a Leica BLK360 imaging laser scanner. The photogrammetric dataset is processed in Agisoft Metashape (Agisoft Metashape, s.f.) to generate a dense point cloud, while the LiDAR dataset is processed using Autodesk ReCap Pro (Autodesk ReCap Pro, s.f.).

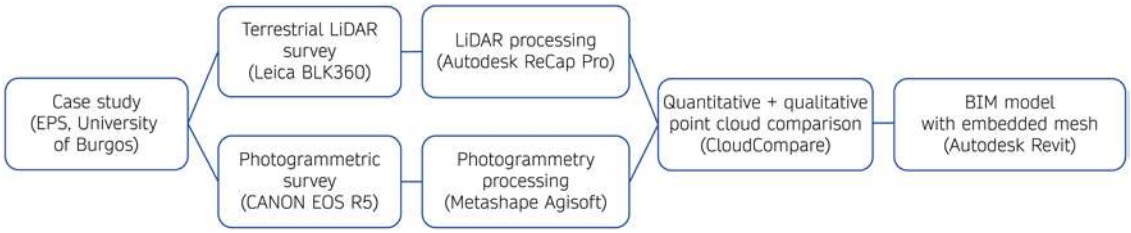


Fig. 1. Pipeline of the proposed methodology (authors' elaboration).

In the point cloud evaluation phase, both datasets are imported into CloudCompare (CloudCompare, s.f.). A manual pre-alignment is performed, followed by fine registration using the iterative closest point algorithm. Once aligned, a cloud-to-cloud distance analysis is conducted to measure geometric differences between the two datasets. This step includes extracting statistical indicators such as mean deviation, standard deviation, and pointwise error distribution.

Following the comparison, the point cloud with the highest geometric quality is imported into Autodesk Revit (Autodesk Revit, s.f.) to begin the 3D reconstruction process. Using the point cloud as a reference, each architectural component is manually modeled as a volumetric element, subdivided into a conformal mesh embedded directly within the modeling process. Finally, the mesh-embedded BIM model is imported into Ansys (Ansys, s.f.), where the quality of the mesh is verified for future FEM-based thermal analysis.

## 3. Experiments

The study focuses on the east-facing façade of the Higher Polytechnic School (EPS) at the University of Burgos in Spain, as shown in (Fig. 2). This wall encloses the offices of university professors. The façade spans approximately 960.00 square meters, covering four floors with a total height of 15.80 meters and a length of 61.00 meters. The composition is segmented into three primary volumes: a central recessed section dominated by curtain wall glazing, flanked by two lateral blocks constructed from exposed aggregate concrete panels. At ground level, a fully glazed corridor

projects slightly forward, creating a sheltered exterior terrace that frames the building's entrance and contributes to its architectural depth.

This façade was selected due to its geometrically complex layout, which combines orthogonal planar walls, large-glazed curtain walls, structural overhangs, and varied textures and materials. Such features are particularly susceptible to distortion or loss of fidelity during 3D reconstruction. Additionally, the presence of shading devices and reflections on glass surfaces presents challenges for both photogrammetric and LiDAR-based capture methods.


Fig. 2. (a, b) Location of the study area (adapted from (Google Earth, s.f.)); (c) East-facing façade selected for analysis (photograph by the authors).

## 3.1. Data acquisition methods

Two separate acquisition sessions were conducted to obtain the necessary point clouds under comparable environmental conditions, approximately 8°C, with low wind and mixed cloud cover, to ensure consistency between datasets. (Table 1) presents a summary of the capture parameters and instruments for both approaches.

Table 1. Summary of data collection.

| Parameter | Photogrammetry | LiDAR |
|---|---|---|
| Equipment | Canon EOS R5 camera, 23mm focal length, f/7.1 aperture, image stabilizer ON, auto-focus; eight-meter aerial photography pole.  | Leica BLK360 imaging laser scanner.  |
| Capture height | 3.70 meters and 4.76 meters (two horizontal rounds). | 3.50 meters placed on the open-air corridor. |
| Acquisition details | 38 photographs, total size 239 MB. Each image resolution: 5,088 x 3,392 pixels. | Point cloud of 13M points; total size: 136 MB. |
| Output format | JPG. | RCS. |
| Capture duration | 00:36:45 (hh:mm:ss). | 00:05:57 (hh:mm:ss). |
| Processing time | 00:13:40 (hh:mm:ss). | 00:05:12 (hh:mm:ss). |

The first dataset was acquired on February 27, 2025, at 09:45 a.m., using terrestrial LiDAR with a Leica BLK360 imaging laser scanner. The device was positioned on the open-air corridor running along the central axis of the building's façade, providing an unobstructed 360-degree line of sight for scanning.

The second dataset was collected on March 3, 2025, at 11:06 a.m., through photogrammetry using a Canon EOS R5 camera equipped with an EF-S 18-55mm lens. The camera was mounted on an eight-meter aerial photography pole to enable both oblique and top-down views. The image acquisition followed a structured grid-like trajectory, executed in two horizontal rounds: one at a height of 3.70 meters and the other at 4.70 meters, as illustrated in (Fig. 3). The camera remained

approximately 10.00 meters away from the façade, with photographs taken every 1.20 meters along the horizontal axis, totaling 19 shots per row and 38 images overall. This setup ensured a minimum lateral overlap of 50% and a frontal overlap between rows of 25–30%.

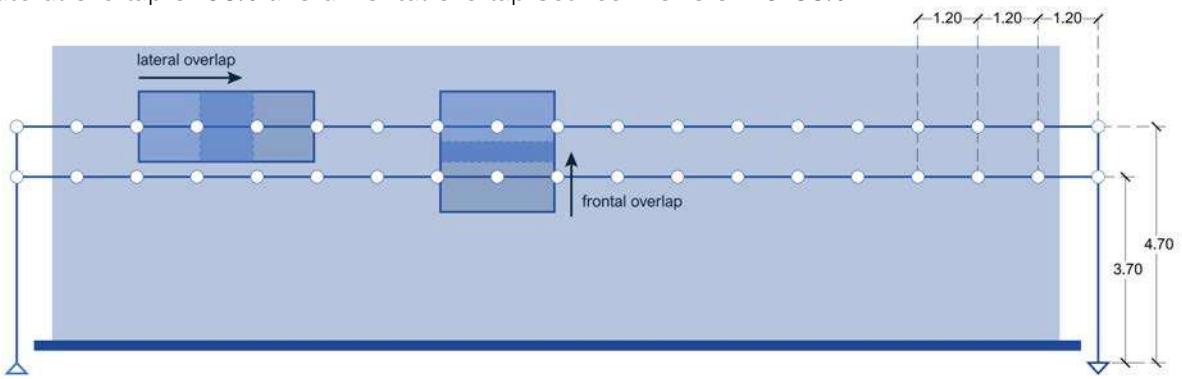


Fig. 3. Photogrammetry capture scheme: image positions (authors' elaboration).

In terms of acquisition and processing time, the LiDAR survey required approximately 5 minutes and 57 seconds for scanning and 5 minutes and 12 seconds for processing. In contrast, the photogrammetric workflow took 36 minutes and 45 seconds for image capture and 13 minutes and 40 seconds for processing (Table 1). Although photogrammetry is generally more accessible and cost-effective, the overall time investment was significantly greater.

### 3.2. Photogrammetric reconstruction

The photogrammetric reconstruction is carried out using Agisoft Metashape (Agisoft Metashape, s.f.) software. The process begins by importing the 38 captured images and executing the *align photos* function, which identifies common features across overlapping photographs to calculate camera positions and generate a sparse point cloud consisting of tie points. This step forms the geometric basis of the model. After alignment, the workflow continues with the build point cloud step, which uses multi-view stereo to create a dense point cloud that captures fine surface detail based on image overlap and depth information. The dense cloud is manually reviewed to eliminate noise.

Following the point cloud generation, the *build model* function is applied to construct a detailed 3D mesh from the depth data. This tetrahedral mesh represents the architectural geometry of the façade as accurately as possible. Finally, the *build texture* step projects the original image data onto the mesh, creating a photorealistic surface finish. The processed point cloud is then exported in LAS, a standardized binary file format developed by the American Society for Photogrammetry and Remote Sensing (A.S.P.R.S., 2011) for the storage and exchange of LiDAR data.

### 3.3. Laser scan processing

The LiDAR dataset is processed using Autodesk ReCap Pro (Autodesk ReCap Pro, s.f.), a software designed for handling and editing large-scale laser-scanned point clouds. Upon importing the raw scan captured by the Leica BLK360, ReCap automatically registers the dataset and visualizes the entire 360-degree environment surrounding the scanning position. This includes not only the target façade but also nearby University buildings, trees, and courtyard elements. Due to the excessive breadth of the scan, the point cloud is manually cleaned to isolate the east-facing façade of the Higher Polytechnic School. No meshing or surface generation is performed at this stage, preserving the dataset in its raw point-based format. Finally, the resulting point cloud is exported in LAS format for the subsequent comparison with the photogrammetric dataset.

### 3.4. Point cloud comparison

This study uses CloudCompare (CloudCompare, s.f.), an open-source 3D analysis tool, to assess the geometric accuracy and alignment between the previously photogrammetric and LiDAR-derived point clouds. Rather than assessing surface coverage, the comparison focuses on the spatial consistency and fidelity of the captured geometries. This evaluation helps determine which dataset offers the most reliable foundation for subsequent modeling and analysis.

The process begins with manually aligning the point clouds using four visually identified reference points common to both datasets. This step ensures that the datasets share a unified spatial reference, enabling meaningful geometric comparison. In this study, the LiDAR point cloud is designated as the reference model, while the photogrammetric dataset is treated as the one to be assessed.

Once aligned, the cloud-to-cloud distance tool is used to calculate the Euclidean distance between each point in the photogrammetric cloud and its nearest neighbor in the LiDAR cloud. This generates a scalar field, where every point in the photogrammetric dataset gets a numerical value corresponding to its spatial deviation from the reference. These values are visualized through a color-coded heatmap, where cooler tones (such as blue and green) indicate minimal differences, and warmer tones (such as yellow and red) highlight areas of greater deviation. The resulting map provides an intuitive visual assessment of the spatial congruence between both datasets.

Alongside the visual output, CloudCompare (CloudCompare, s.f.) also calculates key statistical indicators, most notably, the mean distance, which reflects the average discrepancy between the two clouds, and the standard deviation, which expresses the variability of these deviations. Lower values in both metrics suggest high geometric precision and alignment, whereas higher values may reveal inconsistencies introduced during the capture or processing stages.

### 3.5. BIM-based modeling with embedded hexahedral mesh

Based on the comparison results, the highest quality dataset is selected for further modeling. The point cloud is imported into Autodesk Revit (Autodesk Revit, s.f.), where a BIM model is manually constructed. A key innovation in this step is the direct embedding of a conformal mesh during the modeling process. Rather than using standard families or applying meshing as a pre-process in simulation software, the model is built element-by-element using a voxel-based logic that respects the geometric integrity required for FEM. The resulting model is then exported and validated in Ansys to confirm the mesh's quality, conformality, and readiness for accurate FEM-based thermal analysis.

## 4. Results

### 4.1. Point clouds

The photogrammetric reconstruction, shown in (Fig. 4), yielded a visually detailed and photorealistic model of the east façade. Metashape (Agisoft Metashape, s.f.) successfully aligned all 38 images and generated a dense point cloud that accurately captured surface textures, fenestration patterns, and material discontinuities. However, areas with strong reflections, such as the curtain wall, exhibited minor artifacts and voids, especially near the glass interface and shadowed recesses. Despite these challenges, the textured model retained high geometric fidelity in planar surfaces and structural features, validating the effectiveness of the aerial pole method and grid-based photo acquisition. The technical summary of the photogrammetric steps is summarized in (Table 2).

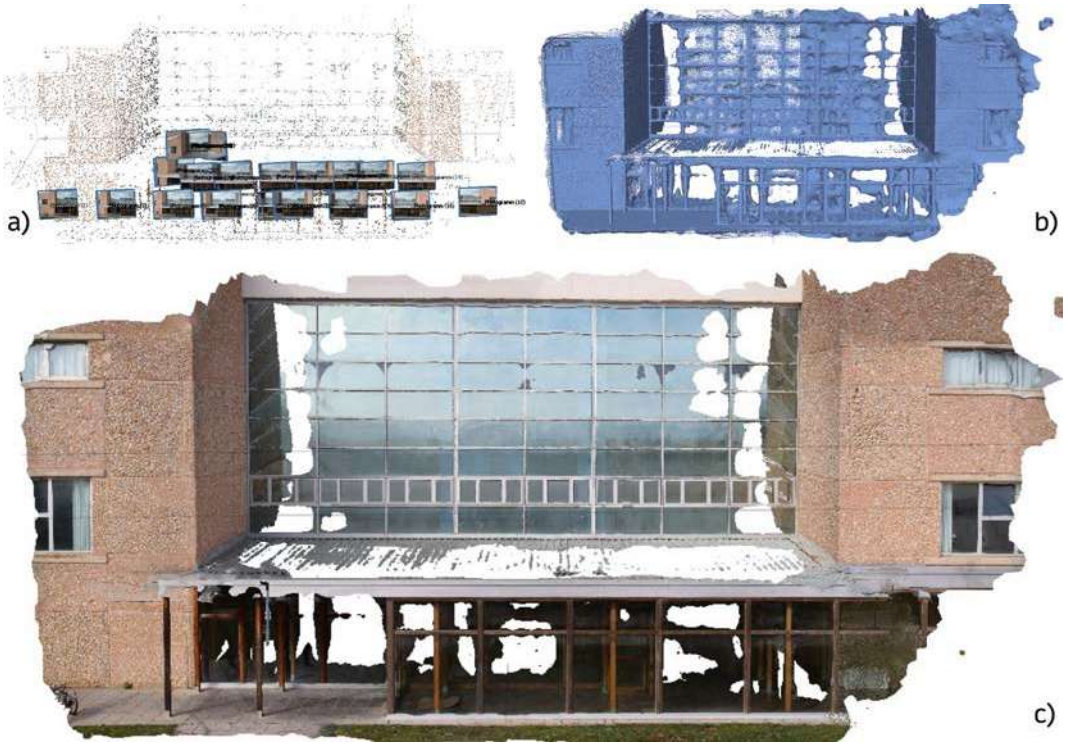


Fig. 4. Photogrammetry reconstruction stages in Metashape: (a) tie points; (b) 3D mesh; and (c) textured model (authors' elaboration).

Table 2. Photogrammetry processing summary in Metashape.

| Step | Key parameters / Output |
|---|---|
| Alignment | 16,242 tie points (Avg. multiplicity: 3.92). Accuracy: Highest. Time: 00:00:25 (hh:mm:ss). |
| Depth maps | 38 maps. Quality: Ultra High. Filtering: Mild. Time: 00:05:52 (hh:mm:ss). |
| Mesh model | 5.8M faces, 2.9M vertices. Surface type: Arbitrary. Time: 00:04:46 (hh:mm:ss). |
| Texture | 8,192 x 8,192 px, Mosaic blending. Time: 00:02:37 (hh:mm:ss). |
| System information | RAM usage: up to 7.55 GB. File size: 341.96 MB. |
| Total processing time | 00:13:40 (hh:mm:ss). |

On the other hand, the laser-scanned point cloud (Fig. 5) captured by the Leica BLK360 imaging laser scanner provided a comprehensive and dense representation of the full scene, including surrounding trees, buildings, and the adjacent courtyard. Once imported into Autodesk ReCap (Autodesk ReCap Pro, s.f.), the dataset required manual filtering to isolate only the east-facing façade. Compared to the photogrammetric model, the LiDAR dataset displayed fewer artifacts around reflective and occluded zones but suffered from occlusions in overhangs and undersides. The resulting point cloud exhibited excellent spatial continuity and provided a reliable geometric reference for later comparison. The technical summary of LiDAR data processing is summarized in (Table 3).

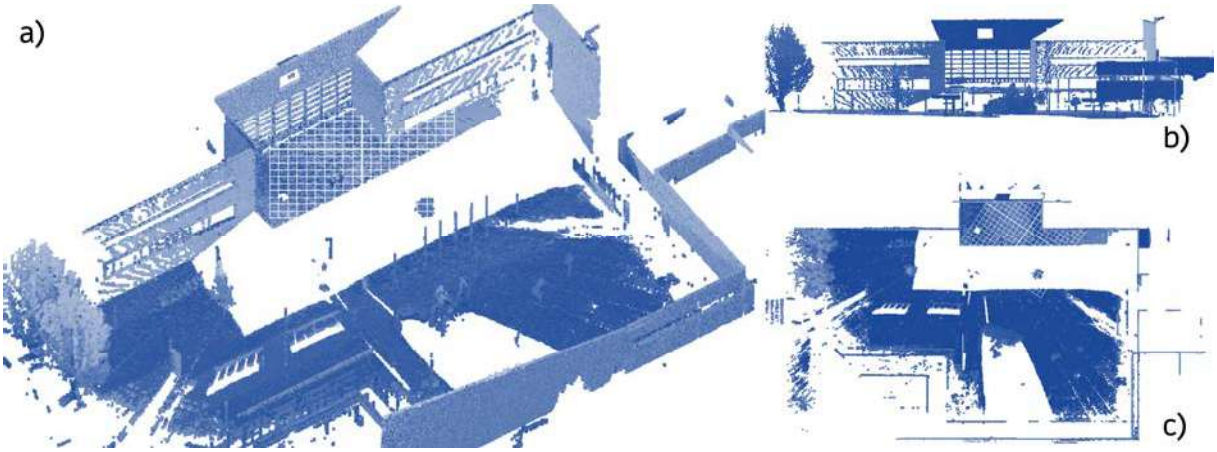


Fig. 5. Geometric reconstruction from LiDAR survey in ReCap Pro: (a) 3D isometric view; (b) orthographic front view; and (c) top view (authors' elaboration).

Table 3. Summary of LiDAR processing.

| Step | Key parameters / Output |
|---|---|
| Import and registration | Single scan. Accuracy: < 6 mm. Importing time: 00:00:07 (hh:mm:ss). |
| Noise filtering | Applied statistical outlier removal. Threshold: 2 SDs. Time: 00:02:15 (hh:mm:ss). |
| Cleaning | Manual crop to east façade. Time: 00:02:50 (hh:mm:ss). |
| Points | Original cloud: 13M. After cleaning: 11M. |
| System information | RAM usage: up to 2.70 GB. File size: 288 MB. |
| Total processing time | 00:05:12 (hh:mm:ss). |

## 4.2. Quantitative geometric comparison

To assess the geometric fidelity of the photogrammetric reconstruction relative to the LiDAR reference, a cloud-to-cloud (C2C) distance analysis was conducted using CloudCompare. The resulting quantitative and qualitative results are presented in (Fig. 6).

The quantitative analysis yielded a near-Gaussian distribution of distances (Fig. 6.a), with a mean absolute deviation of approximately 0.14 meters and a standard deviation of 0.13 meters, across 98 analyzed samples. This indicates that, on average, points from the photogrammetric model deviate by approximately 0.15 meters from their nearest LiDAR counterparts. Additionally, the histogram revealed a left-skewed distribution, with 45.91% of point distances clustered below 0.15 meters and 72.02% below 0.20 meters, indicating generally strong spatial correlation. A secondary peak appears around 0.25 meters, potentially corresponding to mismatches in repetitive textures or reflections on glass. Lastly, the histogram revealed outlier spikes with deviations above 0.50 meters, accounting for only 1.51% of the total point.

The qualitative analysis served to visually localize the areas of deviation across the photogrammetric model, helping identify where the most significant discrepancies occurred relative to the LiDAR reference. The color-coded heatmaps (Fig. 6.b, c) show that flat wall regions and frontal building surfaces exhibited strong alignment, with most of the surface rendered in blue to green tones. These color regions represent deviations within the 0.25-meter threshold used for visualization; however, the actual point-wise deviations in these zones are below 0.10 - 0.15 meters. These low-error regions suggest robust spatial agreement between the datasets in well-lit, planar areas.

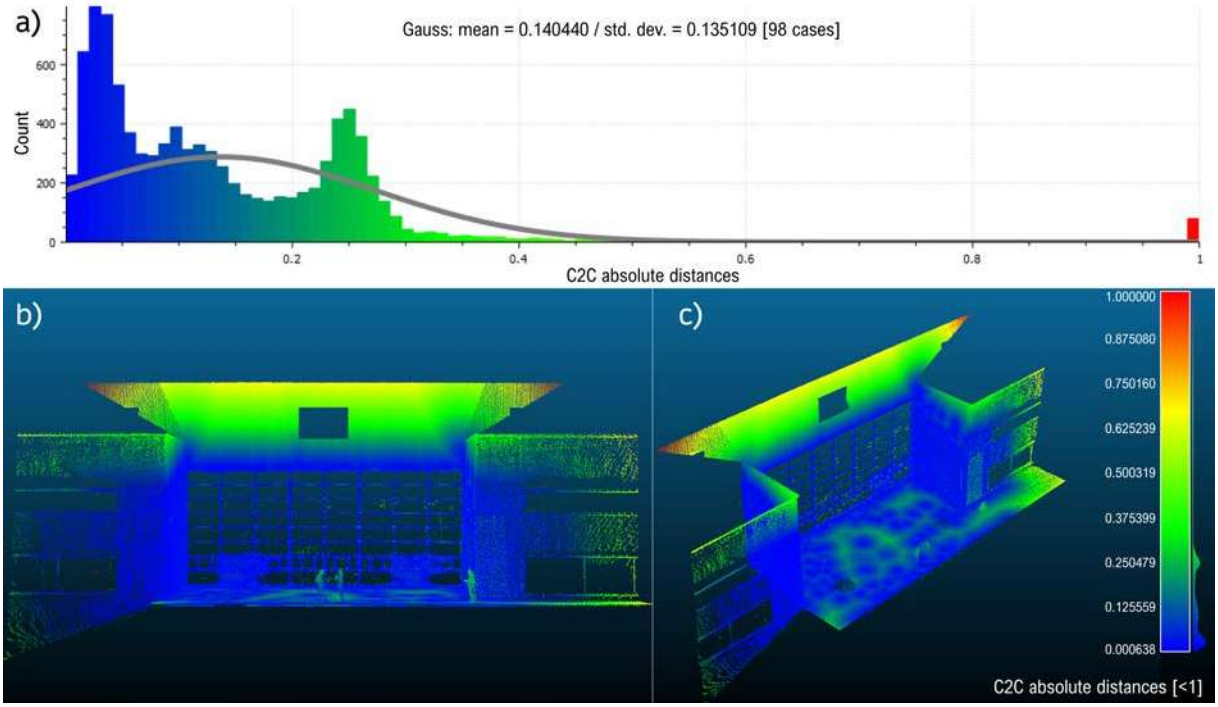


Fig. 6. Geometric deviation analysis in CloudCompare using LiDAR data as reference: (a) histogram showing mean and standard deviation; (b) front view; and (c) isometric view (authors' elaboration).

In contrast, higher deviation areas (shown in yellow and red) were found primarily along reflective surfaces such as windows, roof overhangs, and the upper frontal wall with the square opening. Additionally, error distribution across the model was asymmetrical, with the right side of the building showing slightly higher deviation values. These problematic points typically occur near façade edges, and may be caused by vegetation, occlusions, or missing geometry.

Overall, the LiDAR-derived model exhibited superior sharpness in fine architectural elements such as window frames, corner edges, and structural joints. The photogrammetric reconstruction, while broadly consistent in volumetric shape and scale, exhibited occasional curvature distortions and surface noise, particularly on flat walls and near detail transitions. These discrepancies suggest that, although photogrammetry offers a viable and accessible method for urban-scale modeling, its precision may be insufficient in high-detail or high-contrast areas without enhanced capture protocols or supplemental control points.

### 4.3. 3D conformal model for FEM

Based on the comparison, the LiDAR dataset was selected as the base for modeling due to its completeness and spatial consistency. The point cloud was imported into Autodesk Revit (Autodesk Revit, s.f.), where a parametric BIM model was manually constructed. The model followed a voxel-based logic to ensure perfect conformality between elements and to facilitate the embedding of a structured mesh. This manual modeling process emphasized geometric fidelity, particularly in the thickness of wall offsets, overhangs, and façade divisions, resulting in a solid geometry that remained simulation-ready without additional post-processing. Moreover, the orthogonal geometry of the building enabled the use of strictly rectangular hexahedral elements.

The resulting CAD model, shown in (Fig. 7), comprised 839 rectangular parallelepipeds representing walls, slabs, and roofs. Additionally, it included 5 windows, detailed with 141 solid elements accounting for both frames and glazing. The glass corridor on the first floor was modeled with 25

solid elements, including 20 wooden columns. Additionally, it included 5 windows, detailed with 141 solid elements accounting for both frames and glazing. The glass corridor on the first floor was modeled with 25 solid elements, including 20 wooden columns.

The final step involved importing the BIM model, which consisted of 1,142 bodies, into Ansys (Ansys, s.f.) for meshing and validation. A mesh was generated using a minimum element size of 1.00 meter and CFD *physics preference*, resulting in a fully conformal hexahedral mesh (Fig. 8). The mesh exhibited no topological errors or non-manifold edges, confirming its readiness for structured FEM thermal simulations.

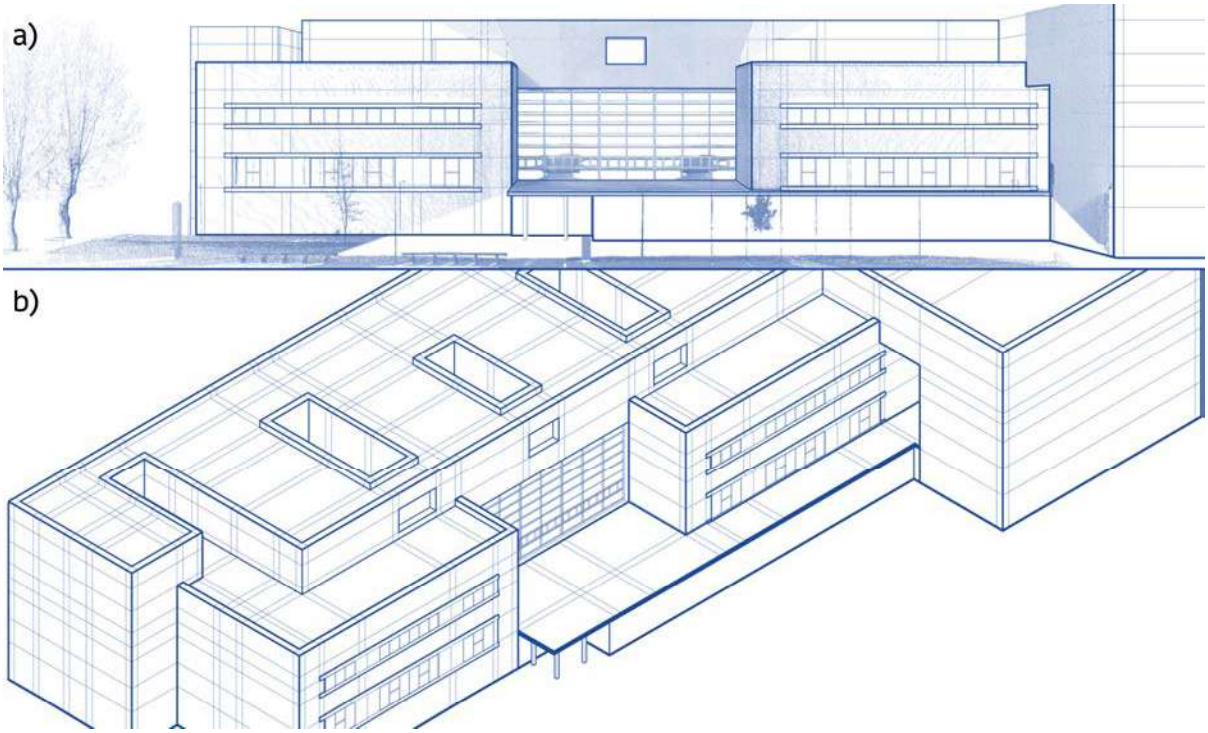


Fig. 7. BIM model creation in Revit: (a) Front view of the manually modeled building with superposed LiDAR point cloud; and (b) Isometric view of the final BIM model with embedded hexahedral mesh (authors' elaboration).

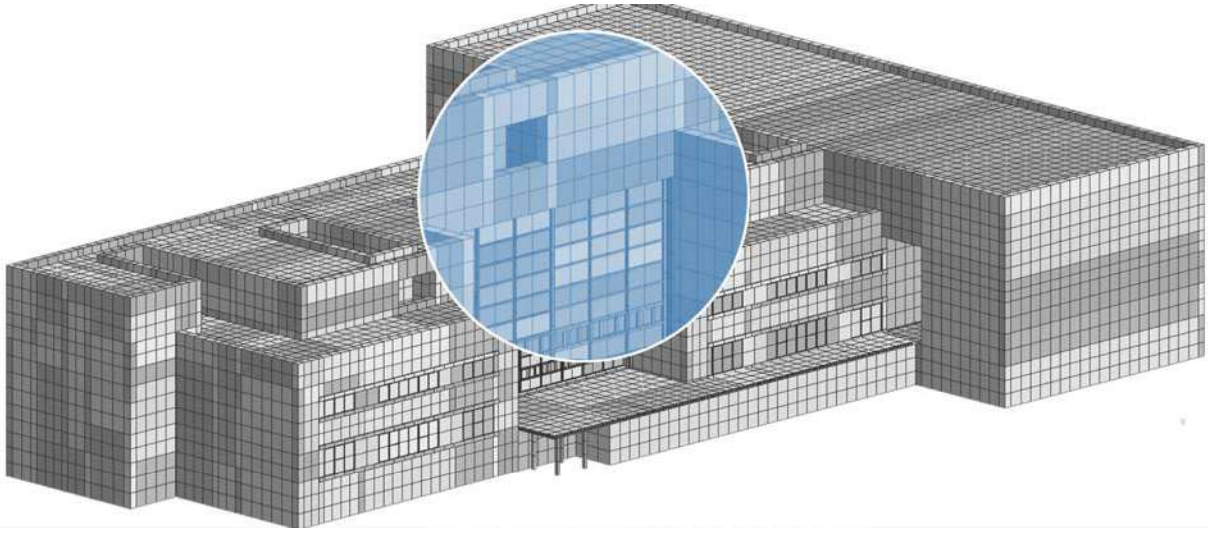

Fig. 8. FEM validation of the BIM model in Ansys (authors' elaboration).

## 5. Conclusions

This study demonstrates a rigorous pipeline for evaluating and processing reality capture data to produce simulation-ready architectural models. By comparing photogrammetry and LiDAR point clouds through quantitative cloud-to-cloud distance analysis, it was able to determine the geometric fidelity of each method and their respective suitability for downstream thermal analysis.

The photogrammetric model delivered high-resolution surface detail and color fidelity. However, it was prone to occlusions and errors in reflective and shadowed regions. In contrast, the LiDAR scan provided a more spatially coherent representation, especially in complex geometries, although it lacked some of the fine visual detail seen in the photogrammetric mesh. Despite these trade-offs, both methods produced viable inputs for 3D reconstruction.

The LiDAR dataset was ultimately chosen as the modeling foundation due to its lower mean error, spatial consistency, and faster acquisition and processing times. Although the building's simplicity could allow for CAD modeling from architectural blueprints alone, real-world conditions often diverge from plans due to undocumented modifications, terrain and vegetation variations, or added elements such as shutters. LiDAR captures these accurately, providing essential boundary condition context, especially for shading analysis.

As a result, a conformal, structured mesh was embedded directly into a manually reconstructed BIM model, streamlining future FEM-based thermal simulation workflows. This approach lays the groundwork for integrating reality capture technologies into robust simulation pipelines, bridging the gap between architectural documentation and performance analysis.

## Funding

This work is part of Projects TED2021-131563B-I00 and PID2022-139477OB-I00 funded by MICIU/AEI/10.13039/501100011033 and, by the “European Union NextGenerationEU/PRTR” and “ERDF A way of making Europe by the European Union”. N. Capetillo thanks to Grant PREP2022-000119 funded by MICIU/AEI/10.13039/501100011033 and by “ESF+” for financial support for her doctoral thesis.

## References

Agisoft Metashape. Retrieved from https://www.agisoft.com

Aguerre, J., et al., (2019). A street in perspective: Thermography simulated by the finite element method. Building and Environment, 148, 225–239. Doi: 10.1016/j.buildenv.2018.11.007

Aguerre, J., et al., (2019). Improving FEM Computations For The Simulation Of Thermograms At The Urban Scale. Building Simulation, 16, 3274–3281. Doi: 10.26868/25222708.2019.210360

Aguerre, J., et al., (2020). Physically Based Simulation and Rendering of Urban Thermography. Computer Graphics Forum, 39(6), 377–391. Doi: 10.1111/cgf.14044

American Society for Photogrammetry and Remote Sensing (2011). LASer (LAS) File Format Exchange Activities. Retrieved from https://www.asprs.org/divisions-committees/lidar-division/laser-las-file-format-exchange-activities

Ansys. Retrieved from https://www.ansys.com

Apollonio, F. I., et al., (2021). A Photogrammetry-Based Workflow for the Accurate 3D Construction and Visualization of Museums Assets. Remote Sensing, 13(3). Doi: 10.3390/rs13030486

Autodesk ReCap Pro. Retrieved from https://www.autodesk.com/es/products/recap

Autodesk Revit. Retrieved from https://www.autodesk.com/es/products/revit

Beckers, B., (2016). Multiscale analysis as a central component of urban physics modeling. Computational Methods in Applied Sciences, 41, 1–27. Doi: 10.1007/978-3-319-27996-1_1

Bouziani, M., et al., (2021). Comparison Assessment Of Digital 3D Models Obtained By Drone-Based Lidar And Drone Imagery. ISPRS Archives, XLVI-4-W5-2021, 113–118. Doi: 10.5194/isprs-archives-XLVI-4-W5-2021-113-2021

Brock, E., et al., (2021). Lidar-Based Real-Time Mapping for Digital Twin Development. IEEE ICME, 1–6. Doi: 10.1109/ICME51207.2021.9428337

CloudCompare. Retrieved from https://www.cloudcompare.org

Google Earth. Retrieved from https://earth.google.com

Guan, S., et al., (2022). A Review on UAV-Based Remote Sensing Technologies for Construction and Civil Applications. Drones, 6(5). Doi: 10.3390/drones6050117

Liu, W., et al., (2024). Digital twin applications in an archaeological site: A virtual reconstruction of the Pishan site, Zhejiang, China. JCAU, 6(1), 1735. Doi: 10.36922/jcau.1735

Muñumer Herrero, E., et al., (2022). Exploring Existing 3d Reconstruction Tools For The Generation Of 3d City Models At Various Lod From A Single Data Source. ISPRS Annals, X-4-W2-2022, 209–216. Doi: 10.5194/isprs-annals-X-4-W2-2022-209-2022

O'Donnell, J., et al., (2019). LiDAR point-cloud mapping of building façades for building energy performance simulation. Automation in Construction, 107, 102905. Doi: 10.1016/j.autcon.2019.102905

Partama, I., et al., (2025). 3D Modeling Using UAV-Photogrammetry Technique for Digital Documentation of Cultural Heritage Buildings. GEOMATE Journal, 28(126), 61–70. Doi: 10.21660/2025.126.4768

Shan, P., et al., (2021). Research on 3D urban landscape design and evaluation based on geographic information system. Environ. Earth Sciences, 80. Doi: 10.1007/s12665-021-09886-y

Waqar, A., et al., (2025). Functional analysis of LIDAR technology in optimizing efficiency and sustainability in construction sector. Ain Shams Engineering Journal, 16(2), 103258. Doi: 10.1016/j.asej.2024.103258

Wibisana, M.., et al., (2024). A LiDAR-Based Digital Twinning Workflow for Traffic Monitoring and Simulation. ISPRS Annals, X-4–2024, 411–418. Doi: 10.5194/isprs-annals-X-4-2024-411-2024

Wolters, C. H., et al., (2007). Geometry-Adapted Hexahedral Meshes Improve Accuracy of Finite-Element-Method-Based EEG Source Analysis. IEEE Transactions on Biomedical Engineering, 54(8), 1446–1453. Doi: 10.1109/TBME.2007.890736

Yucel, B., et al., (2024). A Comparative Analysis of Point Clouds Acquired from UAV Photogrammetry and UAV-based LiDAR in Built Environment. Proceedings of 60th Annual Associated Schools of Construction International Conference, 5, 584–574. Doi: 10.29007/hr8w

Zhang, S., et al., (2024). Guided by model quality: UAV path planning for complete and precise 3D reconstruction of complex buildings. International Journal of Applied Earth Observation and Geoinformation, 127, 103667. Doi: 10.1007/s00371-022-02532-z